Optimization of All-Optical 2R Regenerators Operating at 40 Gb/s: Role of Dispersion

Prashant P. Baveja, Drew N. Maywar, *Member, IEEE*, and Govind P. Agrawal, *Fellow, IEEE*

***Abstract*—We investigate numerically the interplay between dispersion and nonlinearity for optimizing the performance of an all-optical 2R regenerator based on self-phase modulation and spectral filtering at 40 Gb/s. By considering the extent of improvement in the Q factor (related to level of noise reduction), we show that the ratio of accumulated dispersion to the maximum nonlinear phase shift can be used to predict the performance of regenerators making use of fibers with very different lengths, dispersions, and nonlinear parameters. Our results show that fiber dispersion plays an important role and needs to be properly optimized. In general, fibers with larger dispersion perform better but require higher input powers. We also study the impact of fluctuations in dispersion from their nominal value and show that their impact is much less severe when fiber dispersion is relatively small.**

***Index Terms*—Optical communication, optical Kerr effect, optical propagation in nonlinear media, optical pulse shaping, optical signal processing.**

I. Introduction

ALL-OPTICAL regeneration is a promising candidate for replacing optoelectronic regenerators that are currently employed in multichannel lightwave systems operating at bit rates of 40 Gb/s or more. At such high bit rates, the optical signal undergoes degradations through sources such as amplified spontaneous emission (ASE), chromatic dispersion, and various nonlinear effects [1]. To restore the signal quality, some optical regenerators make use of a nonlinear process within a highly nonlinear fiber (HNLF) designed to enhance the nonlinear effects. Indeed, optical regenerators have been made making use of self-phase modulation (SPM)[2], four-wave mixing [3], nonlinear optical loop mirrors [4], and two-pump parametric processes [5] in HNLFs.

Among various regenerator configurations, the 2R regenerator based on SPM-based spectral broadening, followed by spectrally offset filtering, has received much attention [6]–[18] owing to the ease of its implementation, scalability to high bit rates and multiple channels [8], and ease with which a retiming stage can be integrated with it to provide a 3R regenerator [9]. Such regenerators are also known as the Mamyshev-type regenerator (MTR), and considerable work has been done to optimize their performance [10]–[15]. Among other things, the impact of residual dispersion [10], ASE noise [11], filter offset [12], and two-photon absorption [13] has been thoroughly investigated, both theoretically and experimentally. Several studies have focused on the optimization of MTR parameters. For example, optimization on the basis of soliton number [14], followed by the experimental proof of principal, demonstrated the dependence of the Q-factor improvement on input parameters such as the peak input power, fiber dispersion, and pulse width. Numerical simulations for MTRs have been used to deduce scaling rules [15] and to show how its performance depends on device and signal parameters [16]. In spite of these studies, much less attention has been paid to the role played by the HNLF dispersion in optimizing the regenerator performance. It has been commented that fiber dispersion affects the launched input power needed for optimum regeneration [14]. It has also been claimed that high normal dispersion of the HNLF improves the regenerative capability of an MTR [17]. In another study [18], spectral offset of the output filter for a given value of pulsewidth has been optimized as function of the accumulated dispersion and the maximum nonlinear phase shift.

In this paper, we investigate numerically the role of the HNLF dispersion in optimizing the performance of an MTR. In particular, we show how the magnitude of fiber dispersion affects the shape of transfer function and the operating point of an MTR. Based on our numerical work, we suggest some design rules that should prove useful in practice. Our paper is organized as follows. After a brief discussion of the MTR principle and the simulation technique in Section II, we present in Section III our results on the scaling rule related to the dispersion and nonlinear parameters of the HNLF used to make the MTR. More specifically, we calculate numerically the MTR transfer function and the extent of Q-factor improvement for three specific MTR configurations. Resilience of an MTR to dispersion variation is studied in Section IV, and the main results are summarized in Section V.

II. Details of the Numerical Scheme

The schematic of a single-stage MTR, first proposed in [2], is shown in Fig. 1. Such a device employs a high-power erbium-doped fiber amplifier (EDFA) to boost the peak power of the incoming noisy signal to the power level (denoted by P_0) that is high enough to cause spectral broadening through the SPM. The amplified signal is first passed through an ASE rejection filter that rejects the out-of-band ASE noise added by the high-power EDFA. The ASE filter is centered at the signal wavelength (λ_0). The bandwidth of the filter is chosen to be

Manuscript received November 21, 2008; revised February 17, 2009. First published April 28, 2009; current version published August 14, 2009. This work was supported in part by the National Science Foundation (NSF) Award Electrical, Communications and Cyber Systems (ECCS)-0822451.

P. P. Baveja and G. P. Agrawal are with the Institute of Optics, University of Rochester, Rochester, NY 14627 USA (e-mail: baveja@optics.rochester.edu).

D. N. Maywar is with the Laboratory for Laser Energetics, University of Rochester, Rochester, NY 14623 USA.

Digital Object Identifier 10.1109/JLT.2009.2017500

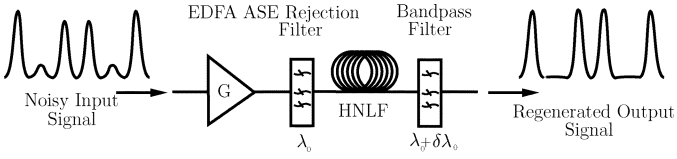

Fig. 1. Components of an MTR. Noise in the output signal is reduced when the signal spectrum, broadened nonlinearly inside the HNLF, is filtered by a bandpass filter that is spectrally offset by $\delta\lambda_0$.

wider than the signal bandwidth [11]. The filtered signal is injected into the HNLF, where it experiences SPM and its spectrum broadens considerably. The HNLF is characterized by its length L, loss α, dispersion D, and the nonlinear parameter γ. The optical bandpass filter (OBPF) placed after the HNLF is offset from the signal wavelength λ_0 by a certain amount $\delta\lambda_o$ so that it lets pass only a slice of the signal spectrum. The bandwidth of the output filter sets the output pulsewidth and needs to be optimized in practice. The filtered signal is a cleaned-up version of the input with reduced noise, but it is offset from the original wavelength by an amount $\delta\lambda_o$.

The propagation of signal through the HNLF is governed by the well-known nonlinear Schrödinger equation

$$\frac{\partial A(z,t)}{\partial z}+\frac{i\beta_2}{2}\frac{^2A(z,t)}{\partial t^2}=i\gamma|A(z,t)|^2A(z,t)-\frac{\alpha}{2}A(z,t) \quad (1)$$

where $A(z,t)$ is the complex amplitude of the optical signal, β_2 is the second-order dispersion parameter, γ is the nonlinear coefficient, and α is the fiber loss.

In the absence of the dispersive effects, (1) can be solved analytically. The result shows that the optical power, $|A(z,t)|^2$, decays as $\exp(-\alpha z)$ because of losses, while the SPM-induced nonlinear phase shift is given by [1]

$$\phi(z,t)=\gamma\int_0^L|A(z,t)|^2dz. \quad (2)$$

A parameter that plays a crucial role for the MTR operation is the maximum nonlinear phase shift ϕ_0 occurring at the center of the pulse where optical power peaks. It is easy to show that

$$\phi_0=\gamma P_0 L_{\text{eff}} \quad (3)$$

where P_0 is the peak input power and $L_{\text{eff}}=(1-e^{-\alpha L})/\alpha$ is the effective HNLF length. The extent of spectral broadening experienced by the signal inside the HNLF depends on ϕ_0.

In the presence of dispersive effects, the spectral broadening inside an HNLF depends both on the nonlinear and dispersion parameters. Since (1) cannot be solved analytically in this case, we solve it numerically using the well-known split-step Fourier method [1]. The nonlinear phase rotation method[19] is used to estimate the required step size.

Our simulations are carried out for a 40-Gb/s signal [in the form of a return-to-zero (RZ) bit stream] with the OptiSystem software (supplied by Optiwave). Fig. 2 shows the block diagram used for numerical simulations. The continuous-wave (CW) laser and the data encoder create the data in the form of a pseudorandom bit sequence consisting of 64 b. Each 1 b contains a Gaussian pulse with a full width at half maximum of 7.5 ps (a 30% duty cycle) at a carrier wavelength of 1550 nm. A white-noise source adds broadband noise to the incoming RZ signal to simulate the degradation of the Q factor associated with the bit stream. This approach is similar to that used in [11]. The bandwidth of the OBPF is adjusted to achieve the desired Q-factor degradation. This filter is a fourth-order super-Gaussian filter with a bandwidth of 1.33 nm. The high-power EDFA has a noise figure of 5.5 dB. The ASE rejection filter shown in Fig. 2 is identical to the OBPF used before the EDFA, and its role is to suppress the ASE noise over the passband of the output offset filter [11], which selects a part of optical spectrum at the output of the HNLF. It is chosen to be a first-order Bessel filter with a spectral width of 0.47 nm and a spectral offset of 0.6 nm. The filtered optical bit stream is converted into an electrical bit stream using a detector, followed with a low-pass Bessel filter with a cutoff frequency of 30 GHz. The resulting electrical signal is used to calculate the output Q factor.

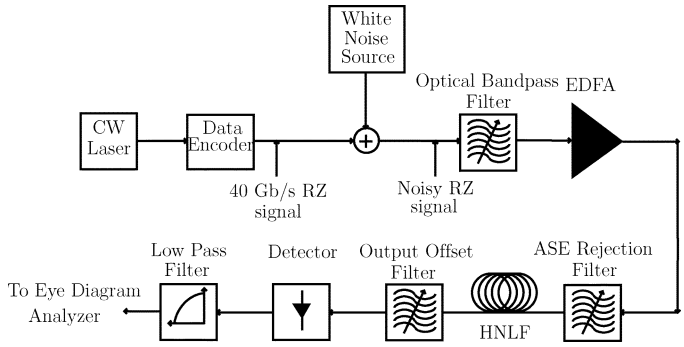

Fig. 2. Setup used for simulating numerically the operation of an MTR.

TABLE I
HNLF PARAMETERS FOR THREE MTR CONFIGURATIONS ANALYZED

MTRs	L (m)	γ (W^{-1}/km)	α (dB/km)	D (ps/nm/km)
MTR 1	1500	5	1	-2
MTR 2	150	50	10	-20
MTR 3	15	500	100	-200

III. ROLE OF DISPERSION AND THE RESULTING SCALING RULE

In this section, we analyze the performance of an MTR by considering the interplay between the dispersive and nonlinear effects taking place simultaneously inside the HNLF and deduce a simple scaling rule. In practice, the HNLF length can vary from a few meters to a few kilometers, depending on the fiber design and material used to fabricate the HNLF. In particular, the required length is much smaller for microstructured fibers because the nonlinear parameter γ is much larger for them. With this in mind, we consider three different types of HNLFs with parameter values listed in Table I.

The choice of fiber parameters for the three HNLFs requires some thought. We have found through extensive simulations that the combined effects of dispersion and nonlinearity on the MTR performance depend on the ratio between accumulated dispersion and maximum nonlinear phase shift defined as $\mathcal{S}=|DL|/\phi_0$ or

$$\mathcal{S}=\frac{|DL|}{\gamma P_0 L_{\text{eff}}}. \quad (4)$$

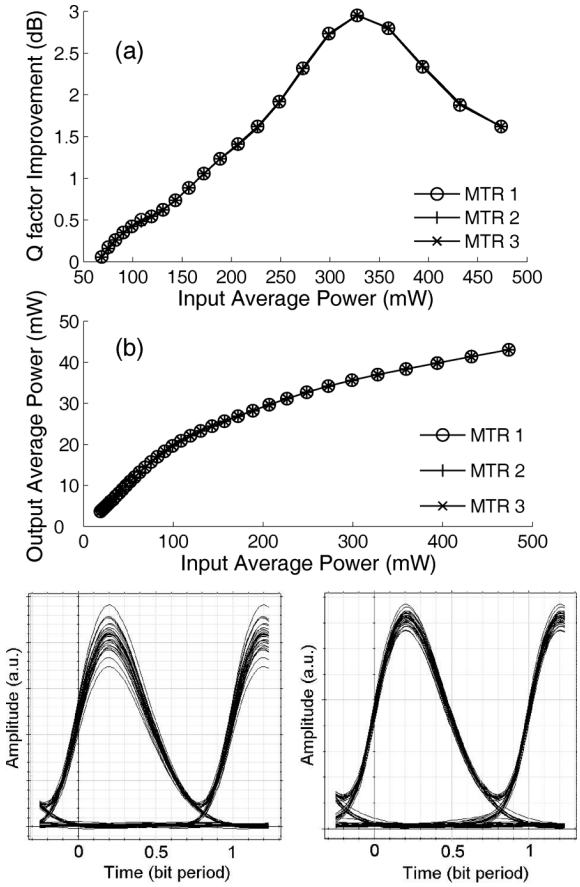

Fig. 3. (a) Improvement in the Q factor as a function of average input power $P_{\rm in}$ and (b) the corresponding transfer function for three MTRs listed in Table I. (c) Input and output eye diagrams for the 40-Gb/s RZ bit stream at the power level corresponding to the peak in part (a).

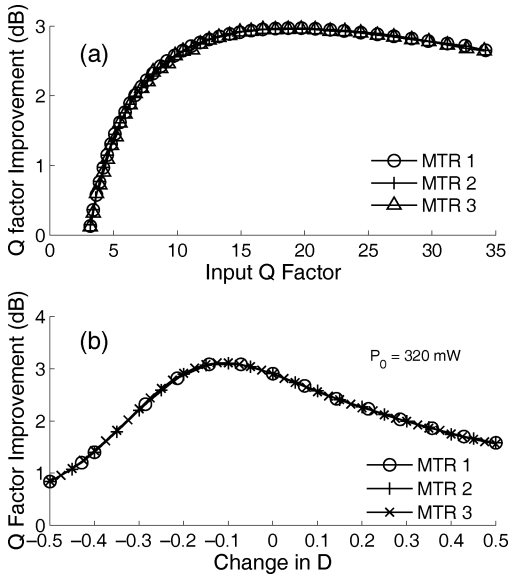

Fig. 4. Improvement in the Q factor (a) as a function of $Q_{\rm in}$ and (b) as a function of δ for three MTRs listed in Table I.

For this reason, we scale in Table I the HNLF dispersion D, nonlinear parameter γ, length L, and loss α by the same factor such that the product DL and ϕ_0, given by (3), remain the same for all the three fibers at a fixed value of the peak power P_0. For the three HNLFs, our new scaling ratio has a value of $\mathcal{S} \approx 0.46\,{\rm ps/km}$ when $P_0 = 1\,{\rm W}$ and scales inversely with P_0.

To show how well the proposed scaling works, we have analyzed the performance of the three MTRs listed in Table I by varying the average input power $P_{\rm in}$ of the 40-Gb/s bit stream from 0 to 500 mW. The corresponding peak power P_0 of the 7.5-ps Gaussian input pulses varied from from 0 to 3 W. The amount of noise added by the white-noise source was controlled to set the input value $Q_{\rm in}$ of the Q factor to 13. For each value of $P_{\rm in}$, we obtain the average output power $P_{\rm out}$ at the exit of the MTR and also calculate the output Q factor. We quantify the improvement in the Q factor by the ratio

$$\Delta Q = 10 \log \left(\frac{Q_{\rm out}}{Q_{\rm in}} \right). \tag{5}$$

Fig. 3(a) shows ΔQ as a function of $P_{\rm in}$ for the three MTRs listed in Table I. The power-transfer functions for the three MTRs are shown in Fig. 3(b). In each case, the three curves almost coincide and cannot be distinguished from each other, indicating that the three MTRs behave in an identical manner in spite of very different HNLFs used inside them. These results provide support for our claim that the ratio between accumulated dispersion and maximum nonlinear phase shift defined by $\mathcal{S}$ introduced in (4) sets the performance of an MTR because it accounts for the interplay between the dispersive and nonlinear effects in a balanced manner. Note that both DL and ϕ_0 have the same values for three MTRs listed in Table I. A much stronger scaling rule will require that they vary such that only their ratio remains unchanged. Our simulations show that such a scaling also holds approximately in the sense that, even though curves similar to those shown in Fig. 3 do not overlap perfectly, they remain close to each other.

Fig. 3(a) shows that the maximum improvement in the Q factor occurs for an optimum value of $P_{\rm in}$ close to 320 mW (or an input peak power P_0 close to 2 W). The maximum nonlinear phase shift for this value is $\phi_0 \approx 13$ and exceeds 4π. Although, in the absence of dispersion, ϕ_0 values of $< 2\pi$ are sufficient to operate an MTR, much larger values are needed when dispersive effects are included. The extent of noise reduction realized at the optimum input power level of 320 mW is evident from Fig. 3(c), where we show the input and output eye diagrams for the 40-Gb/s RZ bit stream.

One may wonder how sensitive our scaling rule is to deviations in the parameter values from those used for Fig. 3. It turns out that our scaling rule is quite robust to such variations. As an example, Fig. 4(a) shows ΔQ as a function of $Q_{\rm in}$ for the three MTRs listed in Table I. Even though ΔQ varies considerably with $Q_{\rm in}$, the three curves again coincide, indicating that the three MTRs behave identically. A rapid decrease in ΔQ for $Q_{\rm in}$ values below 6 shows that an MTR becomes less effective if the input bit stream becomes too degraded. A similar behavior has been observed in earlier studies [16].

Next question we ask is how much the performance of a regenerator changes when D deviates from its value listed in Table I. We quantify the magnitude of relative change in the D parameter by a dimensionless ratio $\delta = (D' - D)/D$, where D' is the modified value of D. Fig. 4(b) shows how ΔQ varies

TABLE II
PARAMETERS FOR FOUR MTR CONFIGURATIONS WITH DIFFERENT HNLFS

MTRs	D (ps/nm/km)	$\delta\lambda_o$ (nm)	Optimum P_0 (W)	$\mathcal{S}$ (ps/nm)
MTR 4	-12	0.61	3.0	0.206
MTR 5	-6	0.61	2.1	0.160
MTR 6	-4	0.37	1.2	0.171
MTR 7	-2	0.37	1.1	0.0935

with δ in the range $-0.5 < \delta < 0.5$. The input average power was kept fixed at 320 mW, a value that corresponds to the peak in Fig. 3(a). As one may expect, ΔQ changes when the dispersion of the HNLF deviates from its original value. However, we found that the Q factor can be improved even beyond the peak value seen in Fig. 3(a) if the dispersion is lower by about 10% compared to the values of D listed in Table I. It appears that there exists an optimum value of D for a given value of the nonlinear parameter associated with an HNLF. Note also that the three curves again coincide in Fig. 4(b), indicating that our scaling rule works even when D changes. The reason is because a change in D just amounts to changing the value of the scaled parameter $\mathcal{S}$ when all other parameters are kept fixed.

IV. IMPACT OF LARGE DISPERSION VARIATIONS

A design question that must be asked is how important is the role of dispersion in realizing optimum performance of an MTR. As mentioned earlier, it has been claimed that high normal dispersion of the HNLF improves the regenerative capability of an MTR [17], but this claim is based on the use of a short-length HNLF with a relatively high value of γ. With the introduction of our scaling parameter $\mathcal{S}$ in Section II, it is evident that large D is required for fibers with high γ to maintain the same value of $\mathcal{S}$. The question then becomes: What is the optimum value of $\mathcal{S}$ for an MTR? We answer this question in this section by considering MTRs with different values of $\mathcal{S}$ and evaluating numerically their relative regenerative capabilities. Table II summarizes the parameter values for four different MTRs that we employ for this purpose. In particular, the values of the nonlinear parameter ($\gamma = 20\,\mathrm{W}^{-1}/\mathrm{km}$), fiber loss ($\alpha = 1\,\mathrm{dB}/\mathrm{km}$), and the fiber length ($L = 250\,\mathrm{m}$) are kept constant, but D is varied from -2 to $-12\,\mathrm{ps}/\mathrm{nm}/\mathrm{km}$. The value of $\mathrm{Q_{in}}$ is set at 13 for the results discussed in this section. The wavelength offset for the output filter was optimized for each configuration, and its optimum value is listed in Table II.

Authors of [15] have employed the shape of the power-transfer function as a predictive measure of the regenerative capacity of an MTR. In particular, they classify different MTRs as type A, B, or C, depending on whether the output power evolves with the input power in a nonmonotonic, locally flat, or monotonic fashion, respectively. Among these, type B is found to be most effective as it tends to equalize the peak power of various 1 b. Fig. 5(a) displays the transfer functions for the four MTRs listed in Table II. From the shape of the curves, we conclude that MTR 4 with $D = -12\,\mathrm{ps}/\mathrm{nm}/\mathrm{km}$ is of type C, while the other three have a locally flat region and may be called Type B. However, these curves do not provide sufficient guidance to let one decide which MTR is the best among the last three, and at what input power level each one should be operated. To answer these questions we have to consider the extent of noise reduction through the improvement in the Q factor.

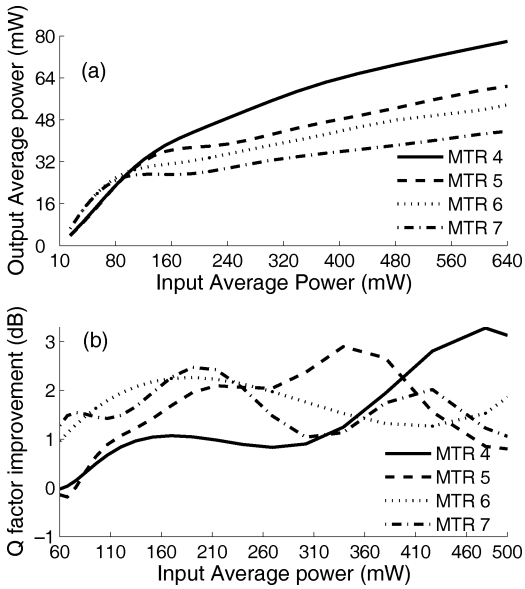

Fig. 5. (a) Power-transfer functions and (b) ΔQ as a function of average input power for the four MTRs listed in Table II.

Fig. 5(b) shows the extent of the Q-factor improvement (ΔQ) as a function of average input power P_{in} for the four MTRs listed in Table II. In each case, ΔQ peaks at a certain input power, indicating that the noise reduction is largest at that power; these values and the resulting values of our scaling parameter $\mathcal{S}$ are listed in Table II. Since the peak value of ΔQ is different for different MTRs, it provides some guidance in picking the best configuration. We must consider another practical matter that is often relevant. In practice, it is desirable that an MTR works at relatively low power levels over as wide range of input powers as possible. We define the operating range of an MTR as the range of P_{in} for which ΔQ exceeds 2 dB. As seen in Fig. 5(b), the required input power is reduced with decreasing D, but the working range of the MTR is also reduced. Thus, a lower value of D allows one to operate at a lower power level, but only at the expense of a reduced operating range and reduced performance because ΔQ is also lower. In contrast, a higher value of D provides a larger value of ΔQ and a wider operating range, but the required input power is also considerably larger. Clearly, a tradeoff exists between the regeneration quality and the average input power required. If input power level is not of much concern, HNLFs with large dispersion provide the best performance.

We also study how sensitive the preceding conclusions are to deviations in the parameter values from those used for Fig. 5. Fig. 6(a) shows ΔQ as a function of Q_{in} for the the four MTRs listed in Table II. Even though ΔQ varies considerably with Q_{in}, the four curves display similar qualitative features. In particular, a rapid decrease in ΔQ for Q_{in} values below 6 shows that an MTR becomes less effective if the input bit stream becomes too degraded. Notice again that the MTR with the largest value of D displays the best performance over a wider operating range. Finally, Fig. 6(b) shows the improvement in the Q factor as a

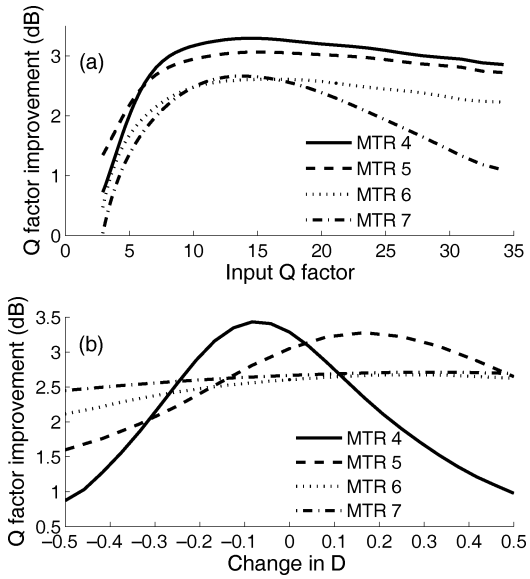

Fig. 6. Improvement in the Q factor (a) as a function of $Q_{\rm in}$ and (b) as a function of δ for the four MTRs listed in Table II.

function of variations in the D value from the value listed in Table II. The most noteworthy feature of this figure is that MTRs with smaller values of D are much more tolerant to variations in the value of the dispersion parameter. This could be attributed to the fact that as the value of $\mathcal{S}$ is lower for MTRs with lower values of D (see Table II). Note that the SPM-induced phase shift and the extent of spectral broadening are also reduced in this case because of the reduced input power at the operating point.

V. Conclusion

We have studied numerically the role of fiber dispersion in improving the regenerative capability of an MTR operating at 40 Gb/s by studying several different MTR configurations. The focus of this work was on the impact of interplay between the dispersive and nonlinear effects that occur simultaneously inside the HNLF used to make the MTR. By considering the extent of improvement in the Q factor (related to level of noise reduction in the 40-Gb/s bit stream), we concluded that a single scaled parameter $\mathcal{S}$, defined in (4) and representing the ratio of accumulated dispersion to the maximum nonlinear phase shift, can be used to predict the performance of MTRs making use of fibers with very different lengths, dispersion, and nonlinear parameters. We then focused on the optimum value of this scaling parameter and varied dispersion over a wide range for a 250-m-long fiber. Our results show that fiber dispersion plays an important role and needs to be optimized in practice. In general, MTRs with larger fiber dispersion perform better but require higher input powers. We also studied the impact of fluctuations in dispersion from their nominal value and found that their impact is much less severe for MTRs designed to operate at a smaller value of $\mathcal{S}$.

Acknowledgment

The support of NSF does not constitute an endorsement of the views expressed in this article.

References

[1] G. P. Agrawal, *Lightwave Technology: Telecommunication Systems*. Hoboken: Wiley, 2005.
[2] P. V. Mamyshev, "All-optical regeneration based on self-phase modulation effect," in *Proc. Eur. Conf. Optical Communication*, Madrid, Spain, Sep. 20–24, 1998, pp. 475–476.
[3] E. Ciaramella and S. Trillo, "All-optical signal reshaping via four-wave mixing in optical fibers," *IEEE Photon. Technol. Lett.*, vol. 12, no. 7, pp. 849–851, Jul. 2000.
[4] A. Bogoni, P. Ghelfi, M. Scaffardi, and L. Poti, "All-optical regeneration and demultiplexing for 160-Gb/s transmission systems using a NOLM-based three-stage scheme," *IEEE J. Sel. Top. Quantum Electron.*, vol. 10, no. 1, pp. 192–196, Jan. 2004.
[5] S. Radic, C. J. McKinstrie, R. M. Jopson, J. C. Centanni, and A. R. Chraplyvy, "All-optical regeneration in one- and two-pump parametric amplifiers using highly nonlinear optical fiber," *IEEE Photon. Technol. Lett.*, vol. 15, no. 7, pp. 957–959, Jul. 2003.
[6] M. Vasilyev and T. I. Lakoba, "All-optical multichannel 2R regeneration in a fiber-based device," *Opt. Lett.*, vol. 30, no. 12, pp. 1458–1460, Jun. 2005.
[7] M. Matsumoto, "Efficient all-optical 2R regeneration using self-phase modulation in bidirectional fiber configuration," *Opt. Exp.*, vol. 14, no. 23, pp. 11018–11023, Nov. 2006.
[8] L. Provost, F. Parmigiani, P. Petropoulos, and D. J. Richardson, "Investigation of simultaneous 2R regeneration of two 40-Gb/s channels in a single optical fiber," *IEEE Photon. Technol. Lett.*, vol. 20, no. 4, pp. 270–272, Feb. 2008.
[9] C. Ito and J. C. Cartledge, "Polarization independent all-optical 3R regeneration based on the kerr effect in highly nonlinear fiber and offset spectral slicing," *IEEE J. Sel. Top. Quantum Electron.*, vol. 14, no. 3, pp. 616–624, May/Jun. 2008.
[10] M. Aoudeh and J. C. Cartledge, "Impact of residual dispersion and ASE noise on the performance optimization of all-optical regenerators utilizing self-phase modulation in a highly nonlinear fiber," *IEEE J. Sel. Top. Quantum Electron.*, vol. 12, no. 4, pp. 717–725, Jul. 2006.
[11] T. N. Nguyen, M. Gay, L. Bramerie, T. Chartier, J. C. Simon, and M. Joindot, "Noise reduction in 2R-regeneration technique utilizing self-phase modulation and filtering," *Opt. Express*, vol. 14, no. 5, pp. 1737–1747, Mar. 2006.
[12] Y. Yang, C. Lou, and D. J. Moss, "Experimental investigation of the influence of filters on regeneration performance in self-phase modulation based regenerator," *Microw. Opt. Technol. Lett.*, vol. 49, no. 1, pp. 192–195, Jan. 2007.
[13] M. R. E. Larmont, M. Rochette, D. J. Moss, and B. J. Eggleton, "Two-photon absorption effects on self-phase-modulation-based 2R optical regeneration," *IEEE Photon. Technol. Lett.*, vol. 18, no. 10, pp. 1185–1187, May 2006.
[14] T. H. Her, G. Raybon, and C. Headley, "Optimization of pulse regeneration at 40 Gb/s based on spectral filtering of self-phase modulation in fiber," *IEEE Photon. Technol. Lett.*, vol. 16, no. 1, pp. 200–202, Jan. 2004.
[15] L. Provost, C. Finot, P. Petropolous, T. Mukasa, and D. J. Richardson, "Design scaling rules for 2R-optical self-phase modulation based regenerators," *Opt. Exp.*, vol. 15, no. 8, pp. 5100–5113, Apr. 2007.
[16] C. Finot, T. N. Nguyen, J. Fatome, T. Chartier, S. Pitois, L. Bramerie, M. Gay, and J. C. Simon, "Numerical study of an optical regenerator exploiting self-phase modulation and spectral offset filtering at 40 Gbit/s," *Opt. Commun.*, vol. 281, no. 8, pp. 2252–2264, Apr. 2008.
[17] M. Rochette, L. Fu, V. Taeed, D. J. Moss, and B. J. Eggleton, "2R optical regeneration: An all-optical solution for BER improvement," *IEEE J. Sel. Top. Quantum Electron.*, vol. 12, no. 4, pp. 736–744, Jul. 2006.
[18] A. G. Streigler and S. Schmauss, "Analysis and optimization of SPM-based 2R signal regeneration at 40 Gb/s," *J. Lightw. Technol.*, vol. 24, no. 7, pp. 2835–2843, Jul. 2006.
[19] O. V. Sinkin, R. Holzlöhner, J. Zweck, and C. R. Menyuk, "Optimization of the split-step Fourier method in modeling optical-fiber communications systems," *J. Lightw. Technol.*, vol. 21, no. 1, pp. 61–68, Jan. 2003.

Prashant P. Baveja received the B.E. degree from Delhi College of Engineering, University of Delhi, New Delhi, India, in 2006. He is currently working toward the Ph.D. degree in optics at the Institute of Optics, University of Rochester, Rochester, NY.

His current research interests include adiabatic wavelength conversion in active resonators, all-optical signal regeneration, nonlinear fiber optics, and Raman amplification.

Drew N. Maywar (S'97–M'06) received the B.S., M.S., and Ph.D. degrees in optical engineering from the Institute of Optics, University of Rochester, Rochester, NY, in 1993, 1997, and 2000, respectively, and the B.A. degree in Religion from the University of Rochester, in 1993.

From 1993 to 1994, he was a Fulbright Scholar at Osaka University's Institute of Laser Engineering. In 2000, he was with Bell Labs, as a Member of Technical Staff, where he codeveloped Lucent's Raman-amplified, 128-channel, dual 10 G-40 G platform, fiber-optic transmission system, LambdaXtreme. In 2003, he joined the Laboratory for Laser Energetics at the University of Rochester as a Scientist, where he is the Lead Laser-System Scientist responsible for the pulse-propagation performance of a nuclear-fusion-enabling 30-TW, 60-beam UV laser, and leads a research group, investigating all-optical signal processing and nonlinear photonic devices. He is the coauthor of 28 research papers published on lightwave communications systems, data-wavelength conversion, all-optical flip-flops, nonlinear optical resonators, and laser-fusion systems, and a book chapter on distributed feedback semiconductor optical amplifiers.

Dr. Maywar is a member of the Optical Society of America (OSA). He was a recipient of a Dissertation Enhancement Award from the U.S. National Science Foundation for photonic-memory research at the University of Tokyo from 1998 to 1999.

Govind P. Agrawal (M'83–SM'86–F'96) received the B.Sc. degree from the University of Lucknow, Lucknow, India, in 1969, and the M.Sc. and Ph.D. degrees from the Indian Institute of Technology, New Delhi, India, in 1971 and 1974, respectively.

After holding positions at the Ecole Polytechnique, France, the City University of New York, New York, and American Telephone and Telegraph Company (AT&T) Bell Laboratories, Murray Hill, NJ, he joined, in 1989, the Faculty of the Institute of Optics, University of Rochester, NY, where he is currently a Professor of optics. He is the author or coauthor of more than 300 research papers, several book chapters and review articles, and seven books entitled: *Semiconductor Laser* (Norwell, MA: Kluwer Academic, 1993); *Fiber-Optic Communication Systems* (Hoboken, NJ: Wiley, 2002); *Nonlinear Fiber Optics* (Boston: Academic Press, 2007); *Applications of Nonlinear Fiber Optics* (Boston: Academic Press, 2008); *Optical Solitons: From Fibers to Photonic Crystals* (San Diego, CA: Academic Press, 2003); *Lightwave Technology: Components and Devices* (Hoboken, NJ: Wiley, 2004), and *Lightwave Technology: Telecommunication System* (Hoboken, NJ: Wiley, 2005). His current research interests include optical communications, nonlinear optics, and laser physics.

Dr. Agrawal is a Fellow of the Optical Society of America (OSA). He is also a Life Fellow of the Optical Society of India. He has also participated multiple times in organizing technical conferences sponsored by the IEEE and OSA. He was the General Cochair in 2001 for the Quantum Electronics and Laser Science (QELS) Conference and a member of the Program Committee in 2004 and 2005 for the Conference on Lasers and Electro-Optics (CLEO).